ChemSearch Journal 10(2): 112 – 122, December, 2019
Publication of Chemical Society of Nigeria, Kano Chapter

Received: 08/10/2019 Accepted: 05/12/2019
http://www.ajol.info/index.php/csj

Reclamation of Malachite Green-Bearing Wastewater Using Desert Date Seed Shell: Adsorption Isotherms, Desorption and Reusability Studies

***Yunusa, U. and Ibrahim, M. B.**
Department of Pure and Industrial Chemistry, Bayero University, P.M.B.3011, BUK, Kano-Nigeria
***Correspondence Email:** umaryunusa93@gmail.com, mbibrahim.chm@buk.edu.ng

ABSTRACT

A low-cost activated carbon adsorbent was prepared from desert date seed shell (DDSS) and utilized for the removal of hazardous malachite green (MG) from aqueous solution using batch mode technique. Different isotherm models were applied to acquire the theoretical data of MG adsorption onto the adsobent at variable initial concentration of 100-1000 mg dm^{-3}. Based on the coefficient of determination (R^2), isotherm models exhibit the following sequence: Freundlich > Langmuir > Redlich-Peterson > Temkin > Jovanovic > Harkin-Jura > Elovich > Dubinin-Radushkevic. The maximum monolayer capacity of the adsorbent was found to be 312.5 mg g^{-1} at 303 K. The mean free energy value (0.91 kJ mol^{-1}) obtained from D-R isotherm suggests that the adsorption process follows physisorption mechanism. Desorption studies for reusability revealed that acetic acid offered the best recovery (52.09%) and the process follow pseudo-second-order kinetics. The conducted reusability test revealed the decline of the adsorbent performance from 96.5% MG removal down to 70.5% MG removal after 5 successive adsorption/desorption cycles.

Keywords: Activated Carbon, Desorption, Isotherms, Malachite Green, Reusability

INTRODUCTION

Dye pollutants present in aqueous systems pose serious threat to the environment recipient. In particular, basic dyes such as malachite green are very difficult to remove due to the presence of aromatic and various functional groups which confer stability to the dye molecules (Mao *et al.*, 2008). Intensely colored effluents from textile, leather, cosmetics, paper and allied industries enter precious water resources deteriorating their quality and consequently intensifying toxicity (Sharma *et al.*, 2017). Hence, the removal of these toxic substances has a significant role in curtailing water pollution.

The hazardous effects of malachite green (MG) have been reported by numerous studies. It is extremely hazardous to mammalian cells and has been identified as a liver tumour promoter (Azaman *et al.*, 2018). MG causes toxicity to respiratory system and damages fertility systems in humans; and is a well-known carcinogenic, mutagenic, and teratogenic substance. Moreover, MG's resistivity to light and reduction due to oxidizing agents are very high. It inflicts lesions on the lungs, skin, eyes, and bones. MG also causes damage to the liver, brain, spleen, kidney and heart (Raval *et al.*, 2017). Therefore, the removal of MG from effluent before been disposed into the waterways is a management serious concern (Tongpoothorn *et al.*, 2019).

Both incineration and land disposal represent likely alternatives for final discard of spent adsorbent material. However, these methods directly or indirectly pollute the environment. Thus, exploring the regeneration and re-use of exhausted adsorbents is imperative to make the adsorption process environmentally friendly and cost-effective. A number of regeneration methods such as chemical, thermal, steam, ultrasound, ozone, oxidative, vacuum, microwave and bioregeneration have been employed to retain the adsorption capacity of spent adsorbents (Momina *et al.*, 2018).

Desert date seed shells (DDSS) are lignocellulosic waste that encounter disposal problem, but are potentially suitable for conversion into low-cost adsorbent. Reported scientific use of this waste are very scanty. The present research was aimed at investigating the effectiveness of activated carbon derived from DDSS as an adsorbent for removal of MG from wastewater. The objectives of the present work, distributed into four parts, were (1) to prepare activated carbon from desert date seed shell via chemical activation with NaOH; (2) to study the equilibrium isotherms of the adsorption process; (3) to carryout desorption studies using different desorbing agents; and (4) to conduct re-usability test of the regenerated adsorbent.

ADSORPTION ISOTHERMS

The adsorption isotherm models are commonly used to design and gain insights about the mechanism of interaction between adsorbent

and adsorbate at equilibrium (Hameed *et al.,* 2008). The models can also provide more information about the capacity of the adsorbent (Labied *et al.*, 2018). In this study, the two-parameter (Langmuir, Freundlich, Harkin-Jura, Temkin, Dubinin-Radushkevic, Jovanovich, Elovich) and three parameter (Redlich-Peterson) isotherm models along with their parameters, which describe the surface interaction and affinity of adsorbent, were used to interpret the equilibrium state for MG adsorption.

Langmuir Isotherm

The Langmuir model is valid for monolayer adsorption onto a surface with finite number of identical sites. The Langmuir isotherm has been commonly used to discuss various adsorbate-adsorbent combinations for both liquid and gas phase adsorptions (Langmuir, 1916). The linear form of this isotherm can be mathematically represented by Eq. 1:

$$\frac{1}{q_e} = \frac{1}{q_{max}.K_L C_e} + \frac{1}{q_{max}} \quad (1)$$

The essential characteristics of Langmuir isotherm can be expressed by dimensionless parameter known as separation factor, R_L, which is defined by Eq. 2 (Mckay *et al.,* 1984):

$$R_L = \frac{1}{(1+K_L C_o)} \quad (2)$$

R_L measures the suitability of the adsorbent for the adsorbate adsorption and it throws light on the nature of adsorption to be either unfavorable (R_L > 1), linear (R_L = 1), favorable (0 <R_L< 1) or irreversible (R_L = 0).

Freundlich Adsorption Isotherm

The Freundlich isotherm is an empirical model that is based on adsorption on a heterogeneous surface (Freundlich, 1906). The Freundlich model can be mathematically presented by Eq. 3:

$$lnq_e = \ln K_f + \frac{1}{n} lnC_e \quad (3)$$

K_F and n are Freundlich constants related with the adsorption capacity and adsorption intensity, respectively.

Temkin Isotherm

Temkin isotherm is the early model describing the adsorption of hydrogen onto platinum electrodes in acidic solutions (Temkin and Pyzhev, 1940). The isotherm contains a factor that explicitly takes into the account of adsorbent–adsorbate interactions. By ignoring the extremely low and large value of concentrations, the model assumes that heat of adsorption (function of temperature) of all molecules in the layer would decrease linearly rather than logarithmically with coverage, as implicit by Freundlich model (Aharoni and Ungarish, 1977). The linear form of the Temkin adsorption isotherm is given by Eq. 4:

$$q_e = B_T lnC_e + B_T lnK_T \quad (4)$$

Dubinin-Radushkevich (D-R) Isotherm

Dubinin–Radushkevich isotherm is an empirical model initially conceived for the adsorption of subcritical vapors onto micro pore solids following a pore filling mechanism (Dubinin & Radushkevich, 1947). The linear form of Dubinin-Radushkevich (D-R) isotherm model is given by Eq. 5-7:

$$lnq_e = lnq_m - \beta \varepsilon^2 \quad (5)$$

$$\varepsilon = RTln\left[1 + \frac{1}{Ce}\right] \quad (6)$$

$$E = \frac{1}{\sqrt{2\beta}} \quad (7)$$

Values of E can predict the characteristics of adsorption as chemisorption or physisorption. If the value of E ranges between 8 to 16 kJ mol^{-1} it depicts the chemisorption nature of adsorption or otherwise physisorption if E < 8 to 16 kJ mol^{-1} (Foo and Hameed, 2010).

Harkin-Jura Isotherm

The Harkin-Jura model assumes the existence of heterogeneous pore distribution on the surface of adsorbents and can be applied to multilayer adsorption (Kausar *et al.,* 2013). This model can be presented Eq. 8:

$$\frac{1}{qe^2} = \frac{B}{A} - \frac{1}{A}\log C_e \quad (8)$$

Where B and A are Harkin-Jura constants obtained from plot of $\frac{1}{qe^2}$ vs $\log C_e$

Elovich Isotherm

This model is based on a kinetic principle which assumes that adsorption sites increase exponentially with adsorption; this signifies a multilayer adsorption (Gubernak *et al.,* 2003). The linear form of the Elovich model is represented by Eq. 9 (Kumara *et al.,* 2010):

$$\ln\frac{q_e}{C_e} = \ln K_{e\,qm} - \frac{q_e}{q_m} \quad (9)$$

Where K_e and q_m are Elovich constant and maximum adsorption capacity respectively and can be obtained from the linear plot represented by Eq. (9).

Jovanovic Isotherm

The model of an adsorption surface considered by Jovanovic is fundamentally the same as that considered by Langmuir, except that the allowance is made in the former for the surface binding variations of an adsorbed species (Jovanovic, 1969). The linear form of this equation is represented by Eq. 10:

$$\ln q_e = lnq_m - K_j C_e \quad (10)$$

Where K_j and q_m are Jovanovic model constants.

Redlich-Peterson Isotherm

The Redlich-Peterson isotherm contains three parameters and combines elements from both Freundlich and Langmuir isotherms (Redlich and Peterson, 1959). Hence, the mechanism of adsorption is a mix and does not follow ideal monolayer adsorption. The linear form of the Redlich-Peterson isotherm can be represented by Eq. 11 (Brouers and Al-Musawi, 2015):

$$\ln \frac{C_e}{q_e} = \beta \ln C_e - \ln(A) \quad (11)$$

Where β and A are Redlich-Peterson constants and can be evaluated from the linear plot represented by Eq. (11).

MATERIALS AND METHODS

Materials

Malachite green dye (purity = 99%) was obtained from E. Merck (Mumbai, India). All other reagents used were of analytical grade. Distilled water was used throughout for the preparation of stock and experimental solutions. An MG stock solution was prepared at 1000 mg dm^{-3} using distilled water and diluted to the desired concentration for each experiment. Solutions were adjusted to desired pH using 0.1 M NaOH or HCl. Desert date fruits were obtained from a local market in Gashua town, Yobe state.

Methods

The preparation of the NaOH activated carbon (NAC) was largely guided by the method described by Wang *et al.* (2014), using a two-step chemical activation technique. Determination of the adsorption capacities for MG by NAC were performed at different initial MG concentrations. In brief, 50 cm^3 of dye solution ranging from 10 to 1000 mg dm^{-3} were added to a set of conical flasks containing 0.3 g of NAC. After agitation (150 rpm) for 60 min at 30°C, the samples were separated by filtration. The residual concentrations of MG were analyzed by UV-Visible spectrometer (Labda 35; Perkin Elmer) at the maximum absorption wavelength (617 nm). The amount of MG adsorbed per unit mass of the adsorbent was calculated by taking the difference between the initial and equilibrium concentrations in solution.

The desorption efficiency of MG-loaded NAC was evaluated in the presence of different desorbing agents; hydrochloric acid (HCl), nitric acid (HNO_3), sulphuric acid (H_2SO_4), acetic acid (CH_3COOH), sodium hydroxide (NaOH) and distilled water. The loaded adsorbent was washed with distilled water to remove traces of unadsorbed MG and dried. Desorption solution (50 cm^3) were added to a set of flasks containing 0.15 g of the MG-loaded adsorbent, followed by agitation at 150 rpm for 60 min. The best desorbing agent was further explored for the effect of contact time (5-120 min) and concentration (0.05-1 M) on desorption efficiency. All analytical methods are the same as above. The reusability of NAC was subsequently evaluated, using the optimal conditions.

Lastly, the NAC was characterized by using Fourier transform infrared spectrometer (Cary 630; Agilent Technologies) to elucidate the functional groups on the adsorbent. Characterization of the NAC was done before and after MG adsorption, over the wave number range of 4000-650 cm^{-1} with a spectral resolution of 8 cm^{-1} and a total number of 32 scans.

RESULTS AND DISCUSSION

Isotherm Studies

Typically, the equilibrium data were analyzed according to the linear forms of the studied isotherms. In order to evaluate the performance of the different isotherms to correlate with experimental data, the plot for each isotherms have been shown in Figs. 1-9, and the evaluated isotherm parameters and correlation coefficient (R^2) are presented in Table 1.

Freundlich Isotherm

Among the studied linear isotherm models, the Freundlich reflected the best fit (R^2, 0.968) to the equilibrium data. The values of K_F (12.47) and the 1/n (0.18) obtained indicate the strength and practicality of the adsorption process respectively. The value of n (5.55) obtained in this study was greater than 1 indicating favourable physical adsorption (Ibrahim, 2011; Azaman *et al.*, 2018). It is worthy of mention that removal of MG by banana peel has also been found to obey Freundlich isotherm (Saechiam and Sripongpun, 2019).

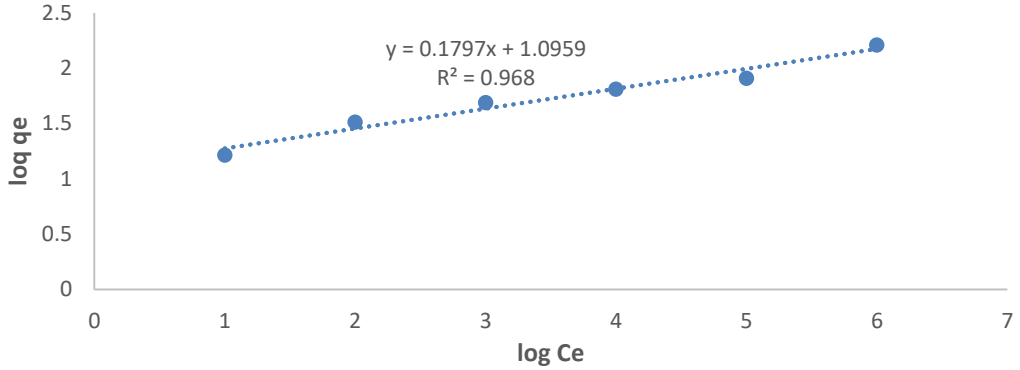

Fig. 1. Freundlich isotherm plot for adsorption of MG onto NAC

Langmuir Isotherm

The Langmuir model (Fig. 2) also show a relatively high correlation coefficient (R^2 = 0.9665). This indicates that the equilibrium data could as well be modelled using the Langmuir isotherm. The computed K_L and maximum monolayer adsorption capacity (q_{max}) of NAC were 0.03 dm^{-3} g^{-1} and 312.5 mg g^{-1} respectively. This indicates the higher affinity and binding capacity of NAC for MG. The value of KL and qmax obtained in this study were higher than values reported for MG adsorption using tea-waste activated carbon (Akar *et* al., 2013). The separation factor (R_L) has also been calculated according to Eq. (2). The values in all the concentrations range studied were in between 0-1 indicating the favorability of MG adsorption on NAC (Labied *et al.*, 2018). It was also observed that R_L values decreased as the initial MB concentration increased indicating that the adsorption process was more favourable at high intial dye concentration (Ahmad *et al*., 2014). The dimensionless separation factor variation with initial loading concentration is as presented in Fig. 3.

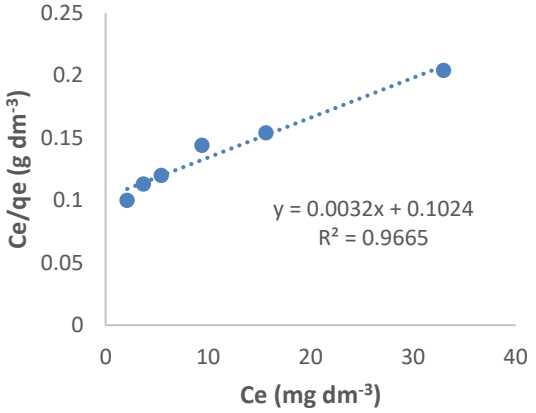

Fig. 2. Langmuir isotherm plot for adsorption of MG onto NAC

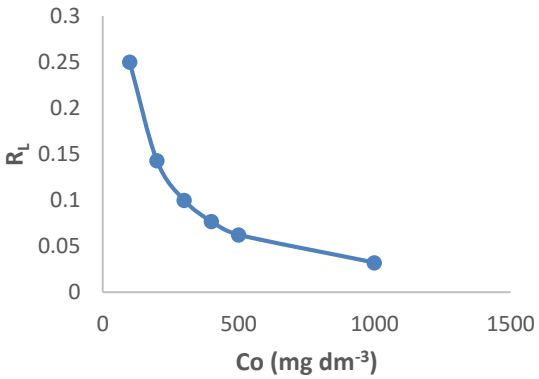

Fig. 3. Plot of separation factor against initial concentration

Dubinin - Radushkevich Isotherm

The Langmuir constants do not explain the chemical or physical properties of the adsorption process. However, the mean free energy (E) obtained from D-R model provides information about these properties (Ushakumary and Madhu, 2014). The D-R correlation coefficient is the lowest (R^2 = 0.6483) as observed from Fig. 4 in comparison with all the studied isotherms. Thus, the D-R model exhibited less fit with the experimental data. The E value (0.91) was less than 8 kJ mol^{-1} implying that the adsorption process is controlled by physical forces. Similar observation was reported for the removal of Congo red using water melon rinds and neem leaves (Ibrahim and Sani, 2014).

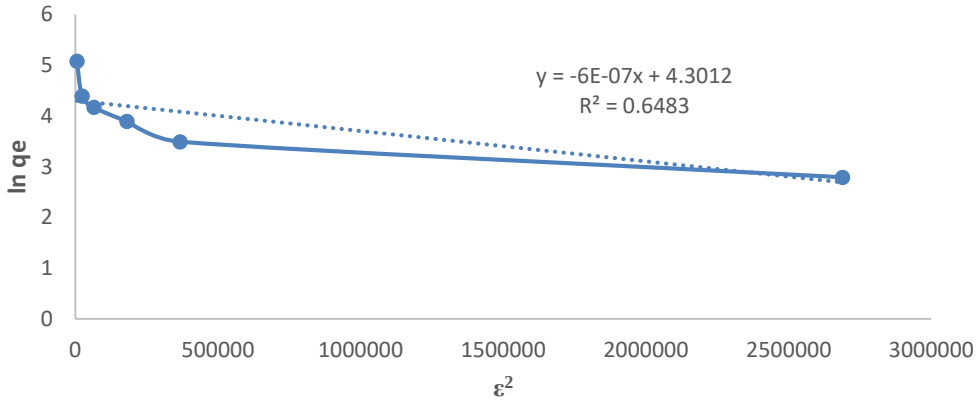

Fig. 4. D-R isotherm plot for adsorption of MG onto NAC

Temkin Isotherm

The heat of adsorption (b) from Temkin isotherm (Fig. 5) is also useful in explaining the nature of binding forces between the adsorbent and adsorbate. Values of b (kJ mol^{-1}) less than 8 signifies that interactive forces are weak and physical in nature whereas values greater than 8 are indicative of strong and chemical interaction (Theivarasu and Mylsamy, 2010). The b values obtained in this study are less than 8 kJ mol^{-1} suggesting the weak interaction between MG and NAC.

Harkin-Jura Isotherm

The Harkin-Jura plot (Fig. 6) as obtained from Eq. (6) depicts isotherm's constants and correlation coefficient as presented in Table 1. The low correlation coefficient value (R^2 = 0.7563) hints that this model does not satisfactorily describe the equilibrium data. Similar results were obtained for the adsorption of picric acid onto carbon nanotubes (Gholitabar and Tahermansouri, 2017).

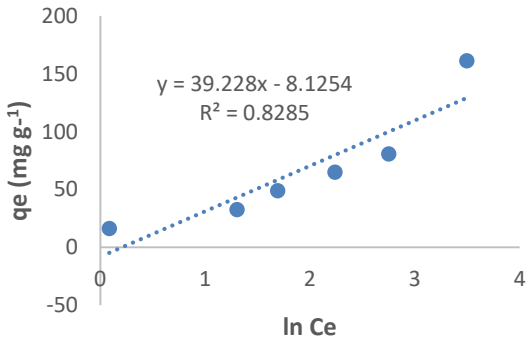

Fig. 5. Temkin isotherm plot for adsorption of MG onto NAC

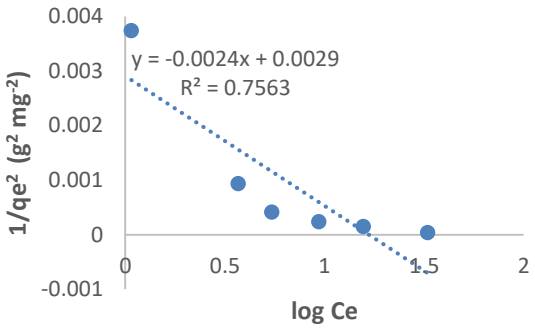

Fig. 6. Harkin-Jura plot for MG adsorption onto NAC

Jovanovic isotherm

The plots of Jovanovic isotherm model is given in Fig. 7 and the parameters calculated from this isotherm are given in Table 1. The value of the correlation coefficient (R^2 = 0.819) from this model shows that it does not satisfactorily explain the experimental data. Similar results were observed for the adsorption of methylene blue by mill fruitis and seeds (Savran *et al*., 2017).

Elovich Isotherm

The Elovich isotherm model for MG adsorption is shown in Fig. 8. The Elovich constants K_E and q_m, are obtained using the linear form of Eq. (8). This isotherm exhibited relatively lower correlation coefficient (R^2 = 0.7059). Furthermore, the q_m values are much lower than the experimental adsorbed amount at equilibrium. Thus, the Elovich model is not sufficient to explain the adsorption of MG onto NAC as similarly observed by Savran *et al*. (2017).

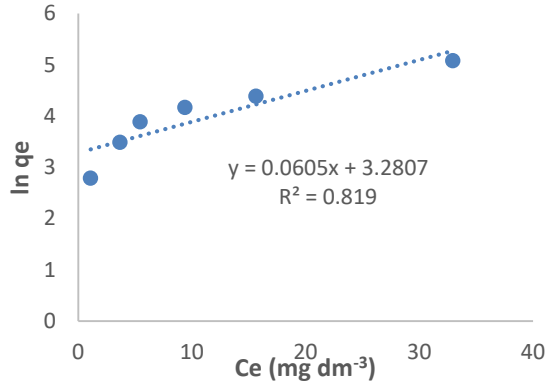

Fig. 7. Jovanovic plot for MG adsorption onto NAC

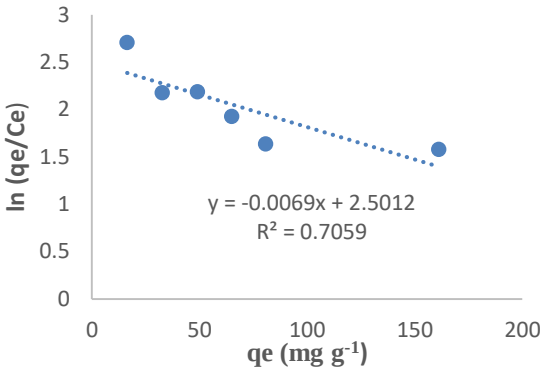

Fig. 8. Elovich plot for MG adsorption onto NAC

Redlich-Peterson Isotherm

The values of Redlich-Peterson isotherm constants are evaluated using the linear form of this model presented Eq. (9) and the values are presented in Table 1. In the light of the relative value of the correlation coefficient, Redlich-Peterson isotherm was found to be also a suitable model for the adsorption of MG owing to its good fitting to the experimental results (R^2 = 0.9638). This observation has been previously reported for the adsorption of hexavalent chromium using *Z. jujube* cores (Labied *et al*., 2018).

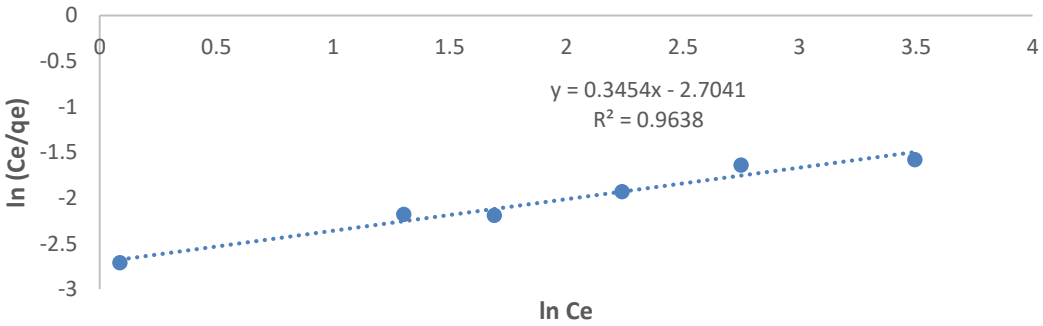

Fig. 9. Redlich-Peterson plot for MG adsorption onto NAC.

Table 1: Isotherm parameters for adsorption of MG onto NAC

Isotherm model	Parameters	Values	R^2	Plot
Langmuir	q_m (mg g^{-1})	312.5		
	K_L (dm^3 mg^{-1})	0.03	0.9665	$\frac{C_e}{q_e}$ vs C_e
	R_L	0.625		
Freundlich	K_F	12.47		
	n	5.55	0.968	$\ln q_e$ vs $\ln C_e$
	I/n	0.18		
Temkin	K_T (dm^3 mg^{-1})	0.81		q_e vs $\ln C_e$
	b (J mol^{-1})	64.12	0.8285	
D-R	q_m (mg g^{-1})	73.79		
	β (mol^2 J^{-2})	6 x 10^{-7}	0.6483	$\ln q_e$ vs ε^2
	E (kJ mol^{-1})	0.91		
Harkin-Jura	B	1.21		
	A	416.66	0.7563	$\frac{1}{q_e^2}$ vs $\log C_e$
Jovanovic	q_m (mg g^{-1})	26.59		
	K_J	0.06	0.819	$\ln q_e$ vs C_e
Elovich	q_m (mg g^{-1})	144.9		
	K_ε	1.02	0.7059	$\ln \frac{q_e}{C_e}$ vs q_e
Redlich-Peterson	β	0.3454		
	A	14.94	0.9638	$\ln \frac{C_e}{q_e}$ vs $\ln C_e$

DESORPTION STUDIES

Selection of Desorbing Medium

To probe the possibility of regeneration of MG-loaded adsorbent, desorption studies was carried out using different regenerants and the results are presented in Fig. 10. The results indicated that acetic acid offered best desorption for MG (33.2%) as also observed by Neupane *et al*. (2014), while NaOH recovered the least (5.6%).

Effect of Concentration

After selection of best desorbing agent (acetic acid), the effects of its concentration on desorption of MG-loaded adsorbents was investigated. The variation in desorption percentage as a function of concentration of acetic acid is given in Fig. 11. It was observed that desorption MG increased with the increase in concentration of acetic acid. Maximum desorption of 52.09% was obtained using 1M acetic acid. At high concentration, the number of hydrogen ions are adequate to replace the MG molecules from the loaded adsorbent. Similar trend was observed in the desorption of MG using concentrations of HCl (Lee *et al*., 2019).

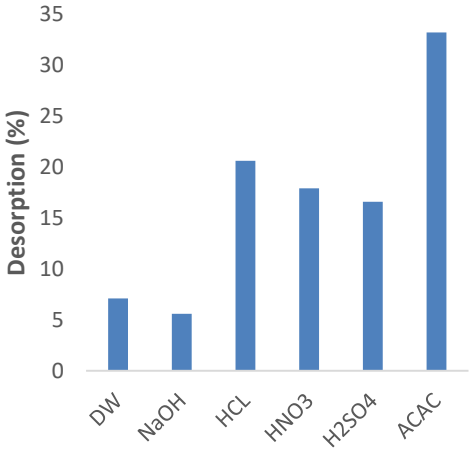

Fig. 10. Selection of desorbing medium

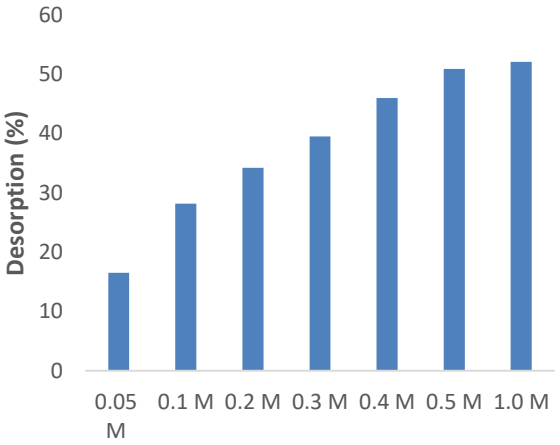

Fig. 11 Effect of concentration of desorbing solution

Effect of Contact Time on Desorption

Batch desorption experiments were carried out for varying time intervals and the result was presented in Fig. 12. It was observed that desorption was rapid in the first 10 min, decreased gradually and reached equilibrium after 30 min. This indicated that the desorption process was quite fast.

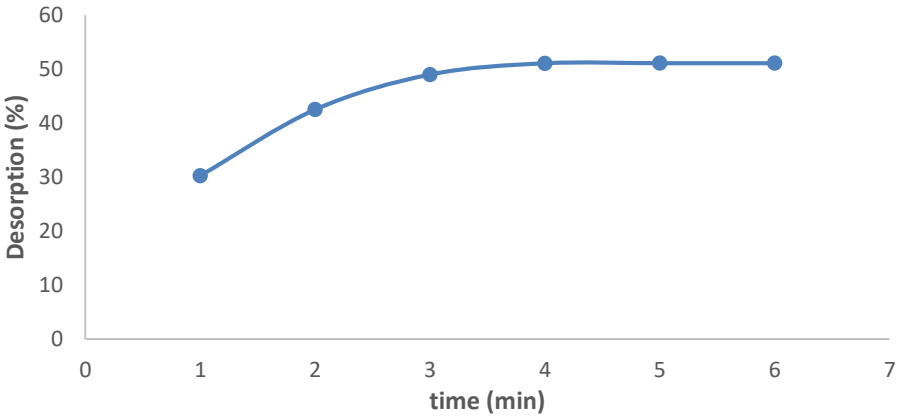

Fig. 12. Effect of contact time on desorption

Desorption Kinetics

Desorption kinetic data obtained were analyzed using different kinetic models and the corresponding parameters are presented in Table 2. The pseudo-second order conforms to desorption of MG based on the relative values of the correlation coefficient (0.9967). Also the theoretical q_d value estimated from the pseudo-second order was 11.11 mg g^{-1}, indicating agreement compared to the experimental values 14.99 mg g^{-1}. Similar behaviour in kinetics was earlier reported for the desorption of hexavalent chromium using NaOH (Yusuff, 2019)

Table 2: Kinetic parameters for desorption of MG from loaded NAC

Kinetic model	parameters	Values
Pseudo-first-order	k_1 (min^{-1})	0.009
	$q_{d\ exp}$ (mg g^{-1})	14.99
	$q_{d\ cal}$ (mg g^{-1})	7.49
	R^2	0.9746
Pseudo-second order	k_2 (g $mg^{-1}min^{-1}$)	0.09
	$q_{d\ exp}$ (mg g^{-1})	14.99
	$q_{d\ cal}$ (mg g^{-1})	11.11
	R^2	0.9967
Intraparticle diffusion	K_{id} ($mgg^{-1}min^{-1/2}$)	1.638
	C	0.8758
	R^2	0.8832
Elovich	β (g mg^{-1})	1.62
	R^2	0.987

Reusability Study

The efficiency of the regenerated adsorbent after five different adsorption/desorption cycles is presented in Fig. 13. It is seen that the adsorption efficiency decreases from 96.5% in the first cycle to 70.5% in the fifth cycle. This hinted that the adsorbent can be successively used for the removal MG from wastewater. The reason for the reduction in adsorption efficiency is because the active sites become fewer after every adsorption-desorption cycle. Similar behavior was reported for the reusability of regenerated cocoa nut shell activated carbon (Azaman *et al*., 2018).

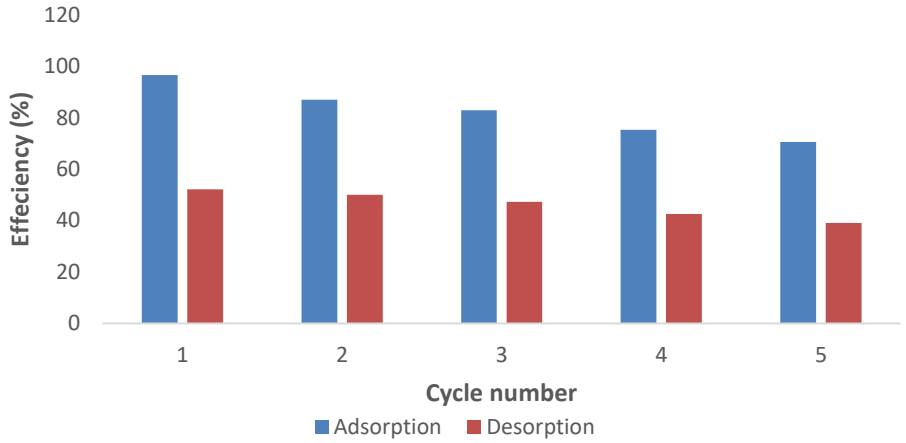

Fig. 13. Efficiency of regenerated adsorbent after five cycles

Functional Group Variation in NAC Before and After MG adsorption

The FTIR spectra for NAC before and after MG adsorption are shown in Fig. 14. Peaks were observed at 3327, 1562, 1447 and 870 cm^{-1} in NAC before adsorption, which were ascribable to O-H stretching, aromatic C-H stretching and free –CSH stretching respectively (Ali *et al.,* 2018; Werkneh *et al.,* 2014). The peak assigned at 3327 cm^{-1} before MG adsorption shifted to 3272 cm^{-1} after adsorption suggesting the formation of intra and intermolecular hydrogen bonds. The FTIR spectrum after adsorption also shows other shifted peak positions and appearance of some new peaks indicating interactions between the adsorbent and MG molecules.

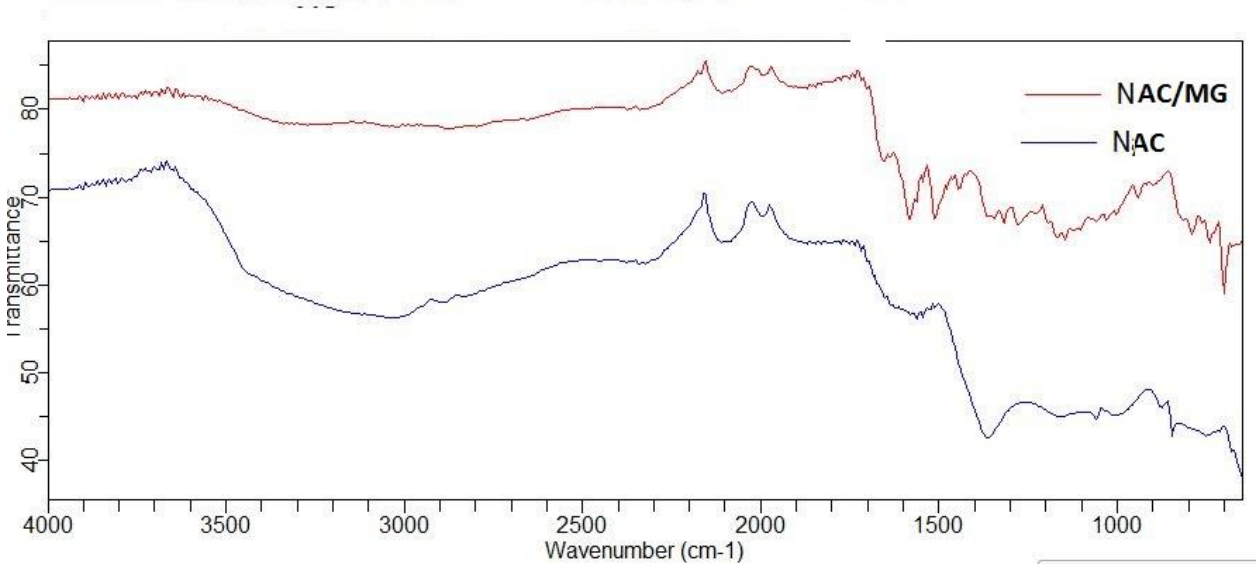

Fig. 14. FTIR spectra of NAC before and after MG adsorption

Comparison of NAC with other Adsorbents

Table 3 summarizes the comparison of the maximum MG adsorption capacities of various adsorbents including NAC. However, the comparison did not account for the experimental variables, different interacting mass-volume ratio and mode of interactions, details of which can be obtained from the respective references. It is obvious from the table that NAC has higher MG adsorption capacity than some previously reported adsorbents in literature.

Table 3: Comparison of maximum adsorption capacities of MG by various adsorbents

Adsorbent	Q_{max} (mg g^{-1})	References
Rice husk	6.5	Muiende *et al.*, 2017
Banana peel	243.9	Saechiam and Sripongpun, 2019
Waste foundry sand	23.29	Gurkan and Koruh, 2018
Napier grass stem	32.27	Tongpoothorn *et al.*, 2019
Malt bagasse	117.65	Reis *et al.*, 2018
Pristine lignin	31.2	Lee *et al.*, 2019
Teak leaf litter powder	333.33	Oyelude *et al.*, 2018
Durian seed carbon	476.19	Ahmad *et al.*, 2014
Coconut shell carbon	214.63	Bello and Ahmad, 2012
Magnetic activated carbon	333.00	Rinku *et al.*, 2015
Oat hull	83.00	Banerjee *et al.*, 2016
Kaolin	128.0	Caponi *et al.*, 2017
Coconut shell carbon	78.11	Azaman *et al.*, 2018
Desert date seed shell carbon	300.2	This study

CONCLUSION

The adsorption and desorption of MG using NAC has been investigated in this study. The NAC has demonstrated good characteristics for removing MG from aqueous solution. The MG adsorption data was well represented by Freundlich, Langmuir and Redlich-Peterson isotherm models although Freundlich isotherm gave the best fit. Acetic acid offered the best recovery for MG among all the studied desorbing agents. NAC has exhibited good reusability properties after five successive adsorption/desorption cycles.

REFERENCES

Ahmad, M. A., Ahmad, N. and Bello, O. S. (2014). Adsorptive Removal of Malachite Green Dye Using Durian Seed-Based Activated Carbon. *Water Air Soil Pollution*. 225:1-18.

Akar, E., Altinisik, A. and Seki, Y. (2013). Using of Activated Carbon Produced from Spent Tea Leaves for the Removal of Malachite Green from Aqueous Solution. *Ecological Engineering* 52: 19– 27.

Ali, I., Peng, C., Khan, Ye, T. and Naz, I. (2018). Sorption of Cationic Malachite Green Dye on Phytogenic Magnetic Nanoparticles Functionalized by 3-Marcaptopropanic Acid. *Royal Society of Chemistry Advances*, 8:8878-8897.

Azaman, S. A. H., Afandi, A., Hameed, B. H. and Mohd Din A. T. (2018). Removal of Malachite Green from Aqueous Phase Using Coconut Shell Activated Carbon: Adsorption, Desorption, and Reusability Studies. *Journal of Applied Science and Engineering*. 21(3):317-330.

Aharoni, C. and Ungarish, M. (1977). Kinetics of activated chemisorption. Part 2. Theoretical Models. *Journal of Chemical Society. Faraday Transaction 1: Physical Chemistry in Condensed Phases*, 73:456-464.

Banerjee, S., Sharma, G.C., Gautam, R. K., Chattopadhyaya, M.C., Upadhyay, S. N., and Sharma, Y. C. (2016). Removal of Malachite Green, a Hazardous Dye from Aqueous Solutions using Avena sativa (Oat) Hull as a Potential Adsorbent. *Journal of Molecular Liquids*. 213:162–172.

Bello, O. S. and Ahmad, M. A. (2012). Coconut (Cocos nucifera) Shell Based Activated Carbon for the Removal of Malachite Green Dye from Aqueous Solutions. *Separation Science and Technology*. 47: 903–912.

Brouers, F. and Al-Musawi, T.J. (2015). On the optimal use of isotherm models for the characterization of biosorption of lead onto algae. *Journal of Molecular Liquids*, 212:46-51.

Dubinin, M.M and Radushkevich, L.V. (1947). The equation of the characteristics curve of the activated charcoal. *Proc. Acad. Sci. USSR Phys. Chem. Sect*. 55:331-337.

Freundlich, H.M.F. (1906). Uber die adsorption in losungen. Z. physical. Chemistry. 57: 385-470

Foo, K.Y. and Hameed, B. H (2010). Insights into the modeling of adsorption isotherm systems. *Chemical Engineering Journal* 156: 2-10.

Gholibatar, S. and Tahermansouri, H. (2017). Kinetic and multi-parameter isotherm studies of picric acid removal from aqueous solution by carboxylated multi-walled carbon nanotubes in the presence and absence of ultrasound. *Carbon Letters*, 22:14-24.

Gubernak, M., Zapala, W. and Kaczmarski, K. (2003). Analysis of benzene adsorption equilibria on an RP-18e chromatographic column. *Acta Chromatographica*, 13:38-59.

Gurkan, E. H. and Coruh, S. (2018). Using Waste Foundry Sand for the Removal of Malachite Green Dye from Aqueous Solutions – Kinetic and Equilibrium Studies. *Environmental Engineering and Management Journal*. 17(1): 123-133.

Hameed, B.H., Tan, I.A.W. and Ahmad, A.L. (2008). *Chemical Engineering Journal*, 144:235 - 244.

Ibrahim, M.B. (2011). Comparative Analysis of the Thermodynamics and Adsorption Isotherms for the Adsorption of Some Metals Ions from Aqueous Solution using Sawdust Material. *Int. J. Res. Chem. Environ*, 1(1):179-185

Ibrahim, M.B. and Sani, S. (2014). Comparative Isotherm Studies on Adsorptive Removal of Congo red from Wastewater by Watermelon Rinds and Neem-Tree Leaves. *Open Journal of Physical Chemistry*, 4(4):139-146

Jovanovic, D. (1969). Physical adsorption of gases.I. Isotherms for monolayer and multilayer adsorption. *Kolloid Z. Z. Polym*, 235(1):1203-1213.

Kausar, A., Bhatti, H.N. and MacKinnon G. (2013). Equilibrium, kinetic and thermodynamic studies on the removal of U(VI) by low cost agricultural waste. *Colloid Surf B Biointerfaces*, 111(124).

Kumara, P.S., Ramalingamb, S., Kiruphac, S.D., Murugesanc, A. and Vidhyarevicsivanesam, S. (2010). Adsorption behavior of nickel (II) onto cashew nut shell in equilibrium, thermodynamics, kinetics, mechanism and process design. *Chemical Engineering Journal*, 1169:122-131.

Labied, R., Benturki, O., Hamitouche, A.Y.E. and Donnot, A. (2018). Adsorption of Hexavalent Chromium by Activated Carbon Obtained from a Waste Lignocellulosic Material (Zizipus jujube cores): Kinetic, Equilibrium and Thermodynamic Study. *Adsorption Science and Technology*, 36(3 - 4):1066 – 1099.

Langmuir, I. (1916). The constitution and fundamental properties of solids and ligiuds. Part I. solids. *Journal of American Chemical Society* 38(11): 2221-2295

Lee, S., Park, J., Kim, S., Kang, S., Cho, J., Jeon, J., Lee, Y., and Seo, D. (2019). Sorption Behavior of Malachite Green onto Pristine Lignin to Evaluate the Possibility as a Dye Adsorbent by Lignin. *Applied Biological Chemistry*, 62(37):1-10.

Mckay, G., Blair, H.S. and Gardiner, J.R. (1984). The adsorption of dyes onto chitin in fixed bed column and batch absorbers. *Journal of Applied Polymer Science*, 29(5):1499-1514.

Mao, J., Won, S.W., Min, J. (2008). Removal of Basic Blue 3 from aqueous solution by Corynebacterium glutamicum biomass: biosorption and precipitation mechanism. *Korean J Chem Eng*, 25:1060-1064.

Momina, Shahadat, M. and Ismail, S. (2018). Regeneration performance of clay-based adsorbents for the removal of industrial dyes: a review. *RSC Advances,* 8:24571-24587.

Neupane, S., Ramesh, S.T., Gandhimathi, R. and Nidheesh, P.V. (2014). Pineapple Leaf Powder as a Biosorbent for the Removal of Crystal Violet from Aqueous Solution. *Desalination and water treatment.* 54(7): 2041-2054.

Oyelude, E.O., Awudza, J. A. M. and Twumasi, S. K. (2018). Removal of Malachite Green from Aqueous Solution using Pulverized Teak Leaf Litter: Equilibrium, Kinetic and Thermodynamic Studies. *Chemistry Central Journal* 12(81):2-10.

Raval, N.P., Shah, P.U. and Shah, N.K. (2017). Malachite Green ‘ a Cationic Dye’ and its Removal from Aqueous Solution by Adsorption. *Applied Water Science,* 7:3407-3445.

Redlich. O. and Peterson, D.L. (1959). A useful adsorption isotherm. *The journal of physical Chemistry,* 63(6):1024-1959.

Reis, H. C. O., Cossolin, A. S., Santos, B. A. P., Castro, K. C., Pereira, G. M., Silva, V. C., Sousa, P. T., Dall’Oglio, E. L., Vasconcelos, L. G. and Morais E. B. (2018). Malt Bagasse Waste as Biosorbent for Malachite Green: An Ecofriendly Approach for Dye Removal from Aqueous Solution. *International Journal of Biotechnology and Bioengineering*. 12(4):118-126.

Saechiam, S. and Sripongpun, G. (2019). Adsorption of Malachite Green from synthetic Wastewater using Banana Peel Adsorbents. *Songklanakarin Journal of Science and Technology*, 41(4):21-29.

Savran, A., Selcuk, N.C. Kubilay, S. and Kul, A.R. (2017). Adsorption Isotherm Models for Dye Removal by *Paliurus spinachristi* Mill Frutis and Seeds in a Single Component System. *Journal of Environmental Science, Toxicology and Food Technology,* 11(4):18-30.

Sharma, K., Vyas, R.K. and Dalai, A.K. (2017). Thermodynamic and kinetic studies of methylene blue degradation using reactive adsorption and its comparison with adsorption. *Journal of Chemical Engineering Data,* 62(11): 3651 – 3662.

Temkin, M.I. and Pyzhev, V. (1940). Kinetics of ammonia synthesis on promoted catalyst. *Acta.phys. Chim. USSR*. 12:327-356.

Thievarasu, C. and Mylsamy, S. (2010). Equilibrium and kinetic adsorption studies of Rhodamine-B from aqueous solution using cocoa (Theobroma cocoa) shell as a new adsorbent. *Int. J. Eng. Sci. Technol*, 2:6284-6292.

Tongpoothorn, W., Somsimee, O., Somboon, T. and Sriuttha, M. (2019). An Alternative and Cost-Effective Biosorbent Derived from Napier Grass Stem for Malachite Green Removal. *Journal of Materials and Environmental Sciences*, 10(8):685-695.

Ushakumary, E.R. and Madhu, G. (2014). Removal of cadmium, chromium, copper, lead, and zinc ions by Alisma plantago aquatica. *International Journal of Environment and Waste Management* 13(1): 75-89.

Wang, X., Wang, S., Yin, X., Chen, J. and Zhu, L. (2014). Activated Carbon Preparation from Cassava Residue Using a Two-Step KOH Activation: Preparation, Micropore Structure and Adsorption Capacity. *Journal of Biobased Materials and Bioenergy*, 8(20):1-8.

Werkneh, A.A., Habtu, N.G. and Beyene, H.D. (2014). Removal of Hexavalent Chromium from Tannery Wastewater using Activated Carbon Primed from Sugarcane Bagasse: Adsorption/Desorption Studies. *American Journal of Applied Chemistry* 2(6): 128-135.

Yusuff, A.S. (2019). Adsorption of Hexavalent Chromium from Aqueous Solution by Leucaena Leucocephala Seed Pod Activated Carbon: Equilibrium, Kinetic and Thermodynamic Studies. *Arab journal of Basic and Applied Science*, 26(1):89-102.